

RELIABILITY AND RISK IMPROVEMENT INDEX AND VALIDATION CRITERIA FOR VENTRICULAR ASSIST DEVICE PROJECTS

Jeferson Cerqueira Dias

Polytechnic School of the University of São Paulo, São, Brasil
ORCID 0055 11 3091-5779

Jônatas Cerqueira Dias

Polytechnic School of the University of São Paulo, São, Brasil
<http://lattes.cnpq.br/7733125441252426>

Rodrigo Lima Stoeterau

Polytechnic School of the University of São Paulo, São, Brasil
<http://lattes.cnpq.br/7354251910888050>

Newton Maruyama

Polytechnic School of the University of São Paulo, São, Brasil
<http://lattes.cnpq.br/6747162018040662>

Paulo Eige Miyagi

Polytechnic School of the University of São Paulo, São, Brasil
<http://lattes.cnpq.br/4019150313777291>

Aron Jose Pazin de Andrade

Instituto Dante Pazzanese de Cardiologia
<http://lattes.cnpq.br/4688924910184370>

Diolino José dos Santos Filho

Polytechnic School of the University of São Paulo, São, Brasil
<http://lattes.cnpq.br/5752765656518774>

All content in this magazine is licensed under a Creative Commons Attribution License. Attribution-Non-Commercial-Non-Derivatives 4.0 International (CC BY-NC-ND 4.0).



Abstract: For Ventricular Assist Device (VAD) projects, a method was developed that can measure, in vitro, the improvement in reliability and risks based on Inherent Safety concept, and criteria for project validation. The samples of VAD used and developed in this research project were VAD.PETG-01 and VAD.PETG-02. The VAD.PETG.01, has a top housing and base that connect to form the pump housing, a magnetic coupling with six magnets that allow external motor drive, and has a bearing shaft clearance adjustment. The VAD.PETG.02 has an impeller, a brushless magnetic rotor with brushless electromagnetic motor, stator, and rolling element bearing rotor and direct drive that allow this internal motor to run. The method, using Fault Tree Analysis, provided the definition of failure frequency of the tested samples which was $5.0014E-02$ (VAD-PETG-01), and $3.314E-03$ (VAD.PETG.02). The failure frequency for the pumps from Reyes' research, used as reference for applying this method, was $1.8228E-05$. Using the failure frequencies of the top events for each sample, the Reliability Improvement Index between samples was calculated (0.068) and the Reliability Improvement was 93.20%. The proposed method presented measurable results of reliability improvement among the tested models, in addition to confirming the acceptability of the Reyes pumps, used as a case study: VAD.PETG.01 and VAD.PETG.02 were plotted in the "unacceptable" region of the Acceptability Criterion, due to the high failure frequency, and Reyes' pumps were plotted in the "acceptable" region. Thereby, the proposed acceptability criterion was consistent with the calculated reliability data.

Keywords: Ventricular Assist Device (VAD), In Vitro, Reliability, Test Bench, Inherent Safety.

INTRODUCTION

According to the International Society for Heart and Lung Transplantation Circulatory Support (IMACS) report of 13,618 continuous flow blood pumps implanted from 2013 to 2016, the number of deaths due to device malfunction was 233, equivalent to 2% (MAVROUDIS; KIRKLIN; DECAMPLI, 2018). Some studies have shown malfunction-related analysis, for example, between HearMate II and HeartWare VADs, which found a higher incidence of HeartWare cases for cable damage and pump thrombosis (SOLTANI et al., 2014). Another study shows an increasing need to detail the subsystems that contribute to device malfunction, indicating 30% controller failure, 19% battery failure (peripheral components), 13% implantable blood pump failure, and 14% of failure in the integral electrical transmission line (KORMOS et al., 2017). The malfunction of the HeartMate III controller (HMIII) was the subject of a study found in the VAD failure survey (MASTORIS; KHASHAB; ABICHT, 2019). Tests on patients with HMIII blood pumps were performed using an electronic stethoscope to detect device failure or thrombosis (SUNDBOM et al., 2019).

In this context, Risk Management can be applied to the VAD project lifecycle for failure identification and treatment (THEISZ, 2015) which, by the way, is urgent. You have a look at the Design History File (DHF; MODARRES; KAMINSKIY; KRIVTSOV, 2017). In this case, the concept of Inherent Safety can be applied in risk analysis to favour an increased reliability (KLETZ; AMYOTTE, 2010). Considering the VAD as an autonomous mechatronic device, the principles of Inherent Safety verified in automation applications can be applied to third class of automatic devices, namely minimization, substitution, moderation and simplification (SUMMERS, 2018). In the project phase of VADs, the use

of the test bench allows monitoring of the device's behaviour during test cycles (REYES et al., 2014).

The aim of this research work is to present a method based on the proposal of a Reliability Improvement Index (RII) and an Acceptability Criterion for the validation and approval of a VAD project. For this, during its project phase, bench tests must be carried out and the data obtained must be collected, so that the method can be applied.

RESEARCH OBJECTIVES

In this context, the general objective of this research project is to propose a methodology for the design of a VAD based on the concept of inherent safety through the definition of a Reliability Improvement Index (RII) and acceptability criterion (AC) capable of measuring the inherent risks of each systems process, associated with the functionality of each subsystem that makes up the Ventricular Assistance System. For this, behavioral variations will be computed over the time of use of this device that may include its life cycle, associated with the risk acceptability of the device and patient safety, proposing the classification of these systems as a class of critical systems.

As a case study, the methodology for samples of VADs will be applied, contemplating the analysis of mechanical subsystems, which are more susceptible to degeneration and failure processes.

In this context, the specific objectives that are intended to be achieved in this research proposal are described below:

- The definition of a method for identifying design and manufacturing failures through a risk analysis process, inspection of geometric, dimensional, and surface requirements for VADs based on test results.
- The definition of a method for identifying functional failures based on the performance of test protocols on VAD test benches.

- A proposed method for quantifying the improvement of reliability and risks with the inherent safety concept applied to the design of a VAD, and a validation criterion for VAD design models.

METHODOLOGY

The methodology for the development of this proposal was based on the definition of a set of activities and the logic of how these activities should be carried out to continuously improve the reliability of VAD projects.

VAD PROJECT AND RISK ANALYSIS METHODOLOGY

The methodology proposed in this work is divided into nine activities for validating a VAD project, as indicated in Fig. 1.

In activity 1 there is the development and review of the VAD project. According to the results of the Risk Analysis, a review and adequacy of the project may be necessary (AYYUB; MCCUEN, 2012).

In activity 2 Risk Analysis, tools are used, according to the level of detail of the project. The causes of hazards, identified during the tests, are systematically analysed using the Ishikawa Diagram. Thus, the recommendations for each identified cause allow a better control of each analysed hazard. One of the concepts introduced here refers to Inherent Safety (LEACH, 2013) of surfaces that have a wellcontrolled topography to affect their function. Examples include the hydrophobic effect of the lotus leaf, the reduction of fluid drag due to the riblet structure of shark skin, the directional adhesion of the gecko foot and the angular sensitivity of the multi-faceted fly eye. Surface structuring is also being used extensively in modern manufacturing industries. Many properties can be altered, for example optical, tribological, biological and fluidic. Previously, single line (profile) (ARAKI et al., 2017). Applying this concept, the recommendations obtained during the Risk

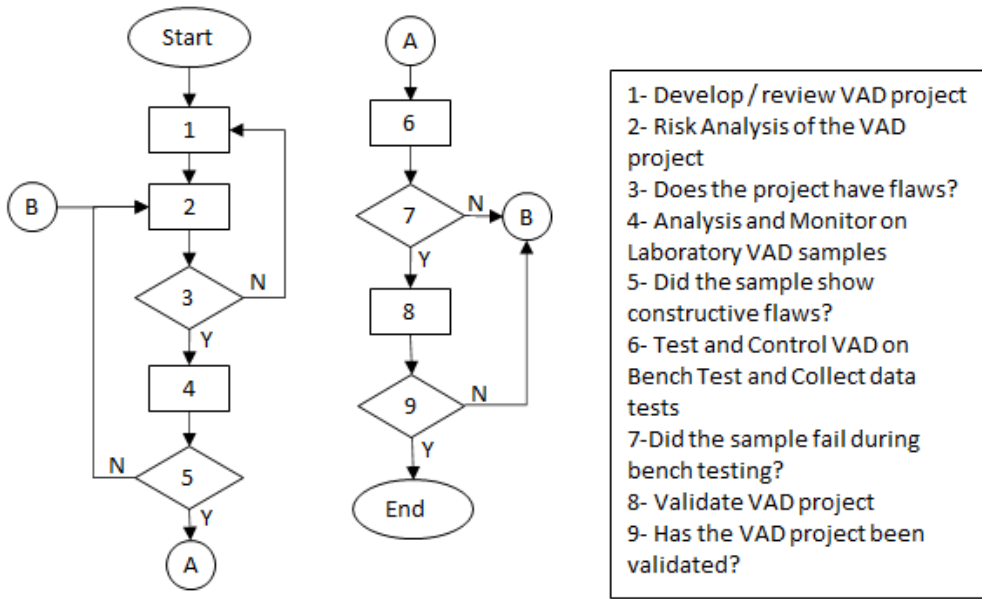


Figure 1. Flowchart of activities for validating a VAD project based on reliability improvement index

Source: Author

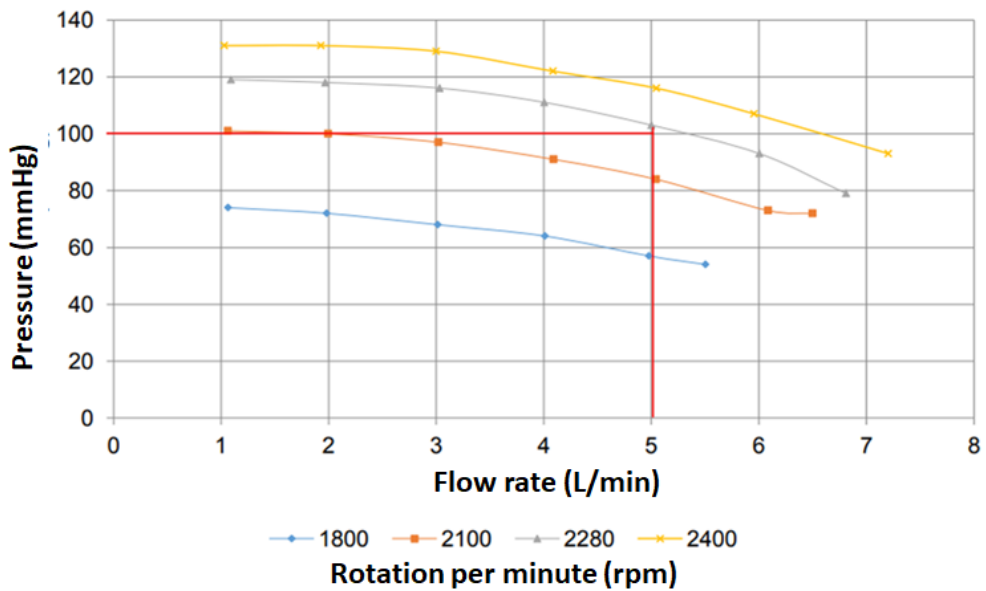


Figure 2 - Hydrodynamic Performance Curve for VAD

Source: Adapted (HERNANDES, 2018)

Analysis must be incorporated into the project, not only as additional safety barriers, but as a review of the project development based on Inherent Safety (RATHNAYAKA; KHAN; AMYOTTE, 2014).

If any conceptual flaw is identified in point 3, it returns to activity 1, where a design review is performed.

Activity 4 indicates the tests that are carried out in the laboratories on geometric, dimensional and/or roughness tests, according to the observed failures. In this activity the prototypes are analysed in relation to their constructive characteristics. 3D roughness analysis indicates failures with defective structural characteristics during fabrication (LEACH, 2013). At this point, the failures identified in point 5 return to activity 2.

In activity 6, the VADs approved in the previous steps are forwarded for bench testing. Samples are subjected to automatic cycles of 50 hours. Bench testing allows for a functional and stress analysis of the device. If any failure is identified in the 50-hour cycle, at point 7, the tested sample returns to activity 2.

During the bench test, data from operational variables, such as flow, pressure, and engine speed, are collected and compared with a hydrodynamic curve, adopted as the standard curve, as shown in Fig. 2. Comparing the curves produced during the tests allows for the identification of deviations in pump performance. This data is stored for future failure trend analysis.

VAD design validation is performed using the graph shown in Fig. 3.

The graph has three regions, acceptable, unacceptable and ALARP (as low as reasonable as possible) (Ayyub, 2011; Modarres, Kaminskiy and Krivtsov, 2017). The validation of the VAD design is based on the failure frequencies accumulated by the number of critical or catastrophic failures identified and calculated. In activity 8, failure frequency data

is plotted for critical or catastrophic failures. In this case, the project will only be approved if the sample presents results plotted in the acceptable region. Projects that present results in the unacceptable region or ALARP will not be validated, so they return to Activity 2 for risk analysis, and, to Activity 1 for project adequacy, as presented in the methodology. The frequency of design failures, indicated in Fig. 3, is obtained by the critical or catastrophic failures that occurred during the bench tests.

Critical or catastrophic failure data are used to calculate the Reliability Improvement Index – RII, according to Equation (1).

$$RII = (1/MTTF_R)/(1/MTTF_A) \quad (1)$$

The RII is a ratio of Recent Mean Time to Failure (MTTFR) to Previous Mean Time to Failure (MTTFP). In this way, it is possible to observe whether the index increases or decreases, showing a ratio between the current VAD project and the previous project.

Once the RII is obtained, the percentage of reliability improvement obtained is calculated using Equation 2.

$$\%RI = 100(1 - RII) \quad (2)$$

The %RI represents the percent of reliability improvement for the project. The RII is a number that varies between 0 and 1. The closer to 0, the better the reliability, as indicated in Equation 3.

$$0 \leq RII \leq 1 \quad (3)$$

CASE STUDY: RISKS ANALYSIS

For the application of the methodology, we sought a case study applied to different samples of VAD produced by prototyping.

DESCRIPTION OF VAD

Ventricular Assistance Device design characteristics

VADs were developed using the design approach to 3D printing and overlaid with precision engineering design rules. The versatility offered by additive manufacturing

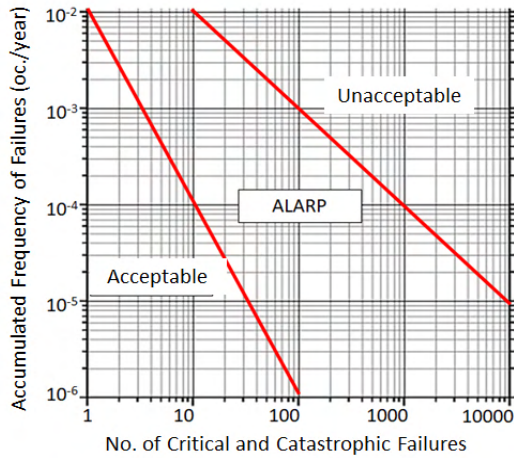


Figure 3 - Acceptability Criteria presented as a Frequency of Failures by the Number of Critical and Catastrophic Failures - "FF-NFCC curve"

Source: Adapted (MODARRES, 2006)

Hazard	Causes	F	S	R	Effect	Recommendation
Bearing Failure	1- Bearing inclination	2	6	12	engine running error	R1.1 Ensure manufacturing as per the design. R1.2 Ensure compliance with the assembly procedure. R1.3 General surface, geometric and dimensional analysis with test protocols.
	2- Clearance between bearing and cradle	1	3	3	Change of pump flow	R2.1 Make mobile cradle base to adjust the lower bearing clearance, with tightening wrench connection, to adjust the clearance. R2.2 Ensure compliance with the assembly procedure.
	3-Deformity in the bearing cradle (manufacturing sheet)	2	3	6	Motor torque friction	R3.1 Ensure fabrication according to design. R3.2 Perform surface, geometric and dimensional analysis with test protocols.
2		6	12	Rotor locking		

Table 1 – Preliminary Hazard Analysis of VAD-AL.01 of Activity "2. Risk analysis"

Source: (DIAS, 2019)

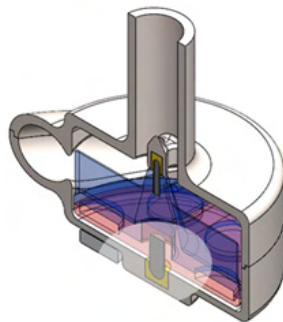


Figure 4 - 3D view of the VAD-PETG.01 VAD model

Source: Prepared by the author (DIAS, 2021)

in terms of generating complex geometries was also explored. This allowed some process limitations to be overcome and the precision needed to operate a VAD. The samples were prototyped in Polyethylene Terephthalate Glycol (PETG).

RISKS ANALYSIS

The risk analysis tool chosen from ISO 31010 was preliminary risk analysis, shown below, applied to each of the models defined for research.

VAD-AL.01 – APR – Qualitative Risk Analysis

The hazard analysis, using the APP tool, presented in Table 1, led to the main recommendations for improving the reliability of the VAD project, applied to the VAD-AL.01 sample.

During Activity execution. Risk Analysis, the danger was identified: “Bill Failure”. Based on this identification, the causes 1, 2 and 3 of this top event was defined like: “Bearing inclination”, “Slack between bearing and cradle” and “Deformity in the cradle of the bearing (manufacturing sheet)”, respectively.

For each of the identified causes, groups of recommendations were determined like: R1 for cause 1, R2 for cause 2, and R3 for cause 3. These recommendations ensure that the top event has its effects - “Motor running error”; “Change of pump flow”; “Friction by motor torque”; “Rotor lockup” - eliminated, neutralized, or reduced.

Thus, the frequencies of these effects can be reduced for future projects if it is ensured that these recommended actions are fully part of the risk management stage proposed in this research project.

VAD-PETG.01 – APR

After the VAD project, sample VAD-AL.01, after implementing the proposed recommendations, according to the previous

analysis, the VAD project, sample VAD-PETG.01, shown in Fig. 4, was obtained. to the Test Bench and a hazard has been identified.

Table 2 presents the results of the Risk Analysis carried out, with the “Wear of moving parts by friction” in the components: rotor, bearing and bearing cradle as an indication of the danger to be resolved. The analysis presented the following causes: “Load on the rotor, bearing and bearing cradle”; “High speed (rpm x volume)”; “Less flow or no pump flow compared to the required flow for the aortic flow” (Required flow); and “Material with inadequate fatigue resistance to the demand of the bearing and bearing cradle” (Bearing and cradle material), identified, respectively, from 1 to 4.

The effects observed for the wear of the moving parts by friction (rotor, bearing and bearing cradle) were: “1- Reduced Mean Time to Failure (MTTF)” when compared to intended; “2- Unexpected stop or lock of the rotor”; “3- Loss of pump performance” (depending on the intended flow); and “4- Hemolysis”. To improve the reliability of the project, measures were proposed to reduce risks and increase reliability based on Inherent Safety, described below: For R1), the recommendations were: “Analyze the volumetry between the rotor blades” and “Update the project with the suggested recommendations”. For R2) the recommendations were: “Develop and analyze pump curves to compare them to numerical models” and “Verify their effectiveness and efficiency”. For R3) the recommendation was: “Analyze the surface and roughness before and after using the VAD, during the bench test, to check for wear”. For R4) the recommendations were: “Analyze the surface and roughness before and after the use of the VAD, during the bench test, to check the wear of the moving parts”, and “Analyze the reduction of failures in relation to the evolution of the wear of the movable parts”. With the implementation of

Hazard	Causes	F	S	R	Effect	Recommendation
Wear of moving parts by friction (rotor, bearing and bearing cradle)	1-Load on rotor, bearing and bearing cradle	2	3	6	1-Mean Time Between Failures (MTTF) reduced	R1.1 Analyze the volumetry between the rotor blades. R1.2 Update the project with the suggested recommendations.
	2-Speed high (rpm x volume)	2	6	12	2-Stop/ unexpected locking of the rotor	R2.1 Develop and analyze pump curves to compare them to numerical models and verify their effectiveness and efficiency.
	3-Lower flow or no pump flow compared to the flow required for the aortic flow	2	3	6	3-Loss of income	R3.1 Analyze the surface and roughness before and after using the VAD, during the bench test, to check for wear.
	4-Material with inadequate fatigue resistance to the demand of the bearing and bearing cradle.	3	4	12	4-Hemolysis	R4.1 Analyze the surface and roughness before and after using the VAD, during the bench test, to check the wear of the moving parts. R4.2 Analyze the reduction of failures in relation to the evolution of wear on moving parts.

Table 2 – Preliminary Hazard Analysis of VAD-PETG.01 of step “2. Risk analysis”

Source: (DIAS, 2019)

these recommendations in the subsequent project, through risk management, it is possible to improve the reliability of the VAD project, in the VAD-PETG.2 model.

VAD-PETG.02

The following effects of the Risk Analysis of the bearing problem or failure were obtained, as shown in Table 1: device rotation error, change in pump flow, friction in motor torque and impeller locking effects. The main causes found were bearing shaft detachment, bearing shaft wear, deformity in the cradle bearing, limitation imposed by the coupling and contact between the pump rotor and the housing. As a solution, the following were recommended: procedures for assembly and operation of the VAD, the modification of the design that could act to reduce friction for a gain in hydrodynamic flow, lower energy consumption and reduce the clearance between the bearing and the bearing cradle. After analyzing the recommendations, the project was revised.

A third VAD project, sample VAD-PETG.02, analyzed using the Preliminary Risk Analysis (PRA) tool is presented in Table 3, part of the “Project Improvement Index Method”.

After the performance tests, the sample presented a “rolling failure” hazard. This time with the use of the PRA for the analysis of “Bearing failure”, the main effects identified were: “Motor rotation error”, “Pump flow change”, “Motor torque friction”, and “Blocking of the motor”. The main causes for bearing failure were: “1- Bearing shaft disengagement”, “2- Bearing shaft wear”, “3- Bearing cradle deformity (manufacturing failure)”, “4-Limitation imposed by coupling (highest rpm)”, and “5-Contact between pump impeller and casing”, respectively. The recommendations have been grouped into R1, R2, R3, R4 and R5. In R1) the recommendations were: “Ensure the production according to the project”; “Ensure compliance with the assembly procedure”; “Geometrical and general dimensional analysis with test protocols”; “Design the fit

to remove the clearance between the bearing and the cradle”; “Project adequacy to reduce the contact force between the cradle and the bearing”. In R2) the recommendations were: “Design the corresponding mobile base of the cradle to adjust the lower bearing clearance with clearance adjustment switch connection”; “Ensure compliance with the assembly procedure”; “Design review to reduce the contact force from the bearing to the cradle”; “post-fabrication qualification, to ensure geometric, dimensional and surface compliance”. In R3) the recommendations were: “Ensure the fabrication in accordance with the project”; “Perform surface, geometric and dimensional analysis with test protocols”; “Design review to reduce bearing to cradle contact force”. In R4) the recommendations were: “Operational procedure to limit rotations”; “Custom project to correct the compatibility between motor speed and magnetic coupling”; “Adequate design to avoid stops and oscillations of the motor in the rotation of the pump rotor”. In R5) the recommendations were: “Design the corresponding mobile base of the cradle to adjust the lower bearing clearance with clearance adjustment switch connection”; “Ensure compliance with the assembly procedure”; “Design review to reduce bearing to cradle contact force”; “To guarantee the

The application of the reliability improvement method allowed an evolution from the initial sample under test VAD-PETG-01 to the sample VAD-PETG-02, where it was possible to apply the concept of Inherent Safety, called minimization, that is, reducing the number of components. The FTA for the VAD-PETG.01, VAD-PETG.02 and VAD-REYES 2014 samples were represented using Bayesian Networks, as shown in Fig. 4. Immediate failures are represented with the portal “or” for the subsystems: SSb-1 Energy, SSb-2 Controller, SSb-3 Driveline,

SSb-4 Motor were inferred from the study by Reyes et al (2014) already mentioned, which resulted in a failure frequency of $3.68E-06$ for each subsystem. The failure frequency of the SSb-5 Pump subsystem obtained during the bench tests for models VAD-PETG.01 and VAD-PETG.02 were $5.0000E-02$ and $3.3334E-03$, respectively. These results impacted the Top Event failure frequencies of each sample which were: $5.0014E-02$ and $3.3480E-03$, respectively. The failure frequency for the Top Event of the VAD-REYES 2014 sample considered for this study was $1.8230E-05$.

VAD TEST BENCH

The test bench, as shown in Fig. 5, used has two tanks (T1 and T2) that allow the transport of fluid between tanks. The bench centrifugal pump has a motor (M1) that ensures a flow between 1.5 L/min up to 9.0 L/min. Sensors for: temperature (TT1), pressure (PT1, PT2, PT3), flow (ST1), rotor speed (VT1), current (IT1, IT2) and valve opening (ZT1) allow monitoring to control operations within desirable operating limits.

The control loop on the test bench allows the programming of test cycles promoting progressive variations in pressure, flow, and rotation on the test bench. The test bench control loop is programmed to perform pressure changes of 26.46 mmHg every 500 seconds. When the cycles reach the time of 4,500 seconds, the programming returns to the initial pressure. The maximum pressure is 220.00 mmHg.

Curve of the VAD-PETG.01 Sample

The Fig. 6 shows the pump curve of the VAD.PETG.01 sample, obtained from the Test Bench. This curve was obtained from a flow valve opening adjustment of 80% and a pump motor power of 90%. The curve is a relationship between pressure (measured in mmHg) and flow (measured in litres per

Problem	Effects	Cause	Solution
Bearing failure	Engine rotation error Change of pump flow Motor torque friction	1.Bearing shaft detachment	R1.1 Ensure the production according to the project.
			R1.2 Ensure compliance with the assembly procedure.
			R1.3 Overall geometric and dimensional surface analysis with test protocols.
			R1.4 Design suitability to remove clearance between bearing and bearing cradle.
			R1.5 Design fit to reduce contact force between cradle and bearing.
	Rotor Locking	2.Bearing shaft wear	R2.1 Match design for movable cradle base to adjust lower bearing clearance with clearance adjustment wrench connection
			R2.2 Ensure compliance with the assembly procedure.
			R2.3 Design overhaul to reduce bearing to cradle contact force
			R2.4 Post manufacturing qualification, to ensure geometric, dimensional, and surface accordance
		3.Deformity in bearing cradle (manufacturing failure)	R3.1 Ensure manufacturing according to design.
			R3.2 Perform surface, geometric and dimensional analysis with test protocols.
			R3.3 Design overhaul to reduce bearing to cradle contact force
		4.Limitation imposed by coupling (higher rpm)	R4.1 Operational procedure for limiting rotations.
			R4.2 Tailor design to correct compatibility between motor speed and magnetic coupling.
			R4.3 Proper design to prevent engine stalls and oscillations in pump rotor rotation.
		5.Contact between pump rotor and housing	R5.1 Match design for movable cradle base to adjust lower bearing clearance with clearance adjustment wrench connection
			R5.2 Ensure compliance with the assembly procedure.
			R5.3 Design overhaul to reduce bearing to cradle contact force
			R5.4 Ensure the production according to the project.

Table 3. Improvement items proposed during phase “2. Risk analysis”

Source: Author

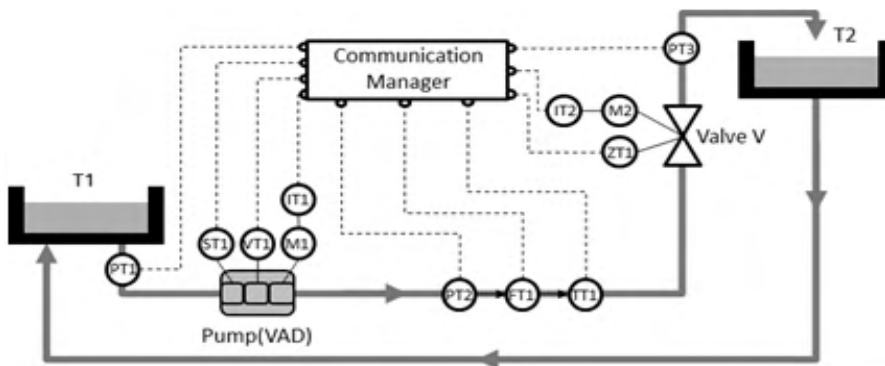


Figure 5. Flowchart of activities for validating a VAD project based on reliability improvement index

Source: Author

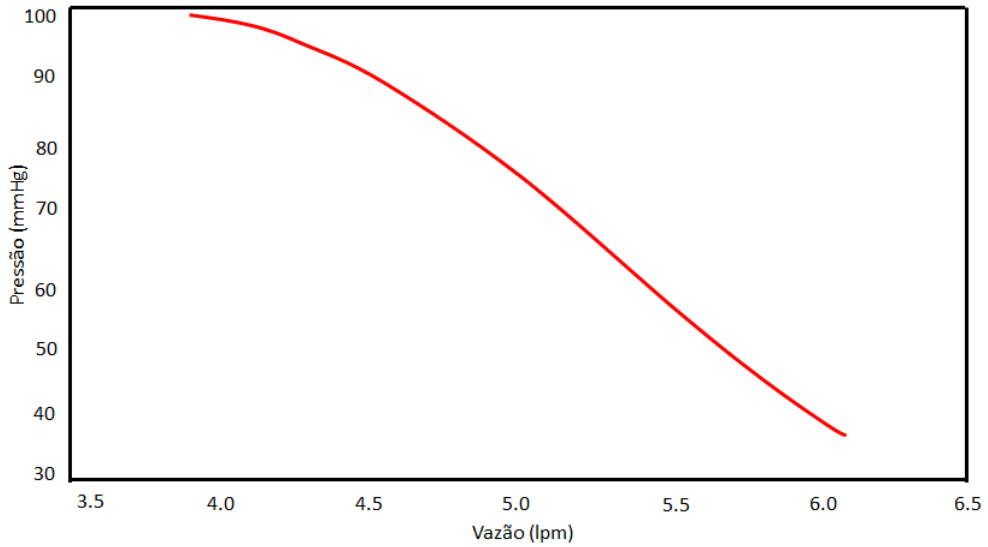


Figure 6 - Pump Curve 80% flow valve opening and 90% engine power - obtained from the Test Bench for sample VAD-PETG.01

Source: Prepared by the author (DIAS, 2021)

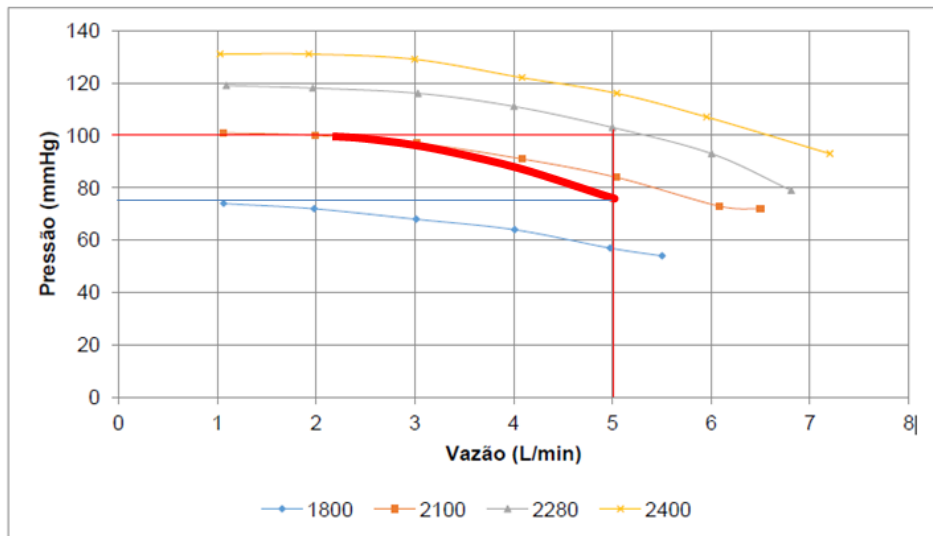


Figure 7 - Comparison between the hydrodynamic performance curve of the VAD (HERNANDES, 2018) and the pump curve of the VAD-PETG.01 sample power 90%

Source: adapted from (HERNANDES, 2018)

minute - lpm). At a flow rate of 4 lpm the pressure is approximately 98 mmHg. And at a flow rate of about 6.2 lpm, the pressure is approximately 38 mmHg.

The curve shown in Fig. 7 is plotted over the standard curve, indicated in red. When compared to the standard curve, it presents a pressure drop equivalent to approximately 10 mmHg between the flow rate of 3.4 lpm and 5 lpm, in the rotation curve of 2100 rpm.

Adequacy of the Project after Risk Analysis

In the new revised project, model VAD-PETG.02, as shown in Fig. 8, the concept of Inherent Safety, minimization, can be observed.

The second prototype, model VAD-PETG-02, was a new binding design based on experiences gained in previous models. All parts except the brushless frameless DC motor were manufactured using a DLP (UV Resin Direct Light Processing) of an Object 24 3D printer. External drive and magnetic coupling were eliminated using a direct drive solution. A frameless brushless DC motor was selected, with the magnetic ring mounted directly on the impeller. This reduced space allowed for an overall size reduction without compromising flow efficiency. The elimination of the magnetic coupling made room for a superior dynamic motor with higher revs.

VAD PROJECT VALIDATION

The analysis for validation of the VAD design models, VAD-AL.01, VAD-PETG.01, and VAD-PETG.02 were developed from Fig. 8. For design validation, it is necessary to determine the Improvement Index of project, obtained from the activity "Calculate the IMPT" indicated in the 2nd level PFS, represented in Fig. 8. As mentioned before, the "IMPT" is a function of the "RIIT" and the "IMCT".

Risk Improvement Index (RII)

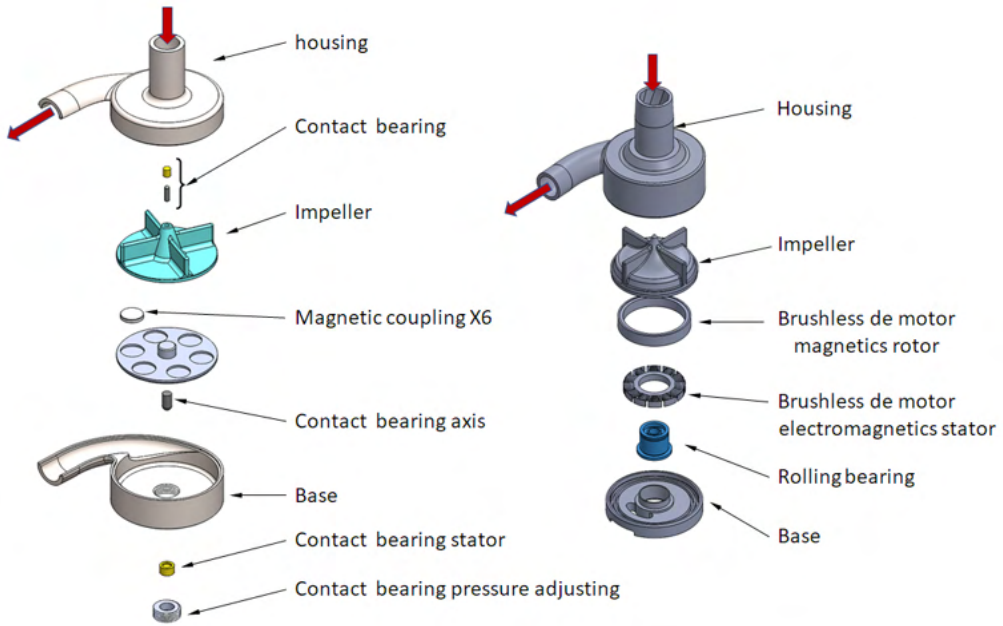
The "RII_T" is obtained from the activity "Calculate the RII_T" which is based on the BowTie analysis tool. The risk improvement index represents a quantitative analysis, using Bayesian Networks for the results of probabilities of occurrence of the final events, between the previous project model and the improvement model.

The RII_T is based on the application of the global calculation of risks, using the Bayesian Networks model to calculate the values obtained from the use of Bow Tie Analysis. On the left side of the diagram, the FTA data are used to determine the TE. As the FTA is of the "or" type, the frequencies are added to determine the TE failure frequency. From the frequency of failures determined for the TE, the probability of success and failure of the safety barriers, on the right side of the TE, represented in the SEA, was used.

The values obtained are here inferred for an application of quantitative analysis, where the hypothesis of 99% success of safety barriers against 1% failure is estimated. To obtain the frequency of each final event, the frequency of failure of the top event was multiplied by the probability of success or failure of each branch until reaching the probability of occurrence of the final event. From the quantitative data in the diagram obtained in the Bow Tie analysis, the calculation for the RIIT was applied. When applying the calculation using the Bayesian Network, the value obtained is the representation of the RII of the tested project.

The Fig. 9 shows a Bow Tie Analysis of the design associated with the VAD-AL.01 sample, with the inferred failure probabilities for subsystems 1 to 4, with subsystem 5, pump, having an actual failure after a test actual 20 hours, which resulted in a failure frequency of 5,000000E-02.

This result impacted the TE failure frequency, 5.001473E-02, which triggered an



a) First Prototype VAD-PETG-01

b) Second Prototype VAD-PETG-02

Figure 8. Design Evolution

Source: Author

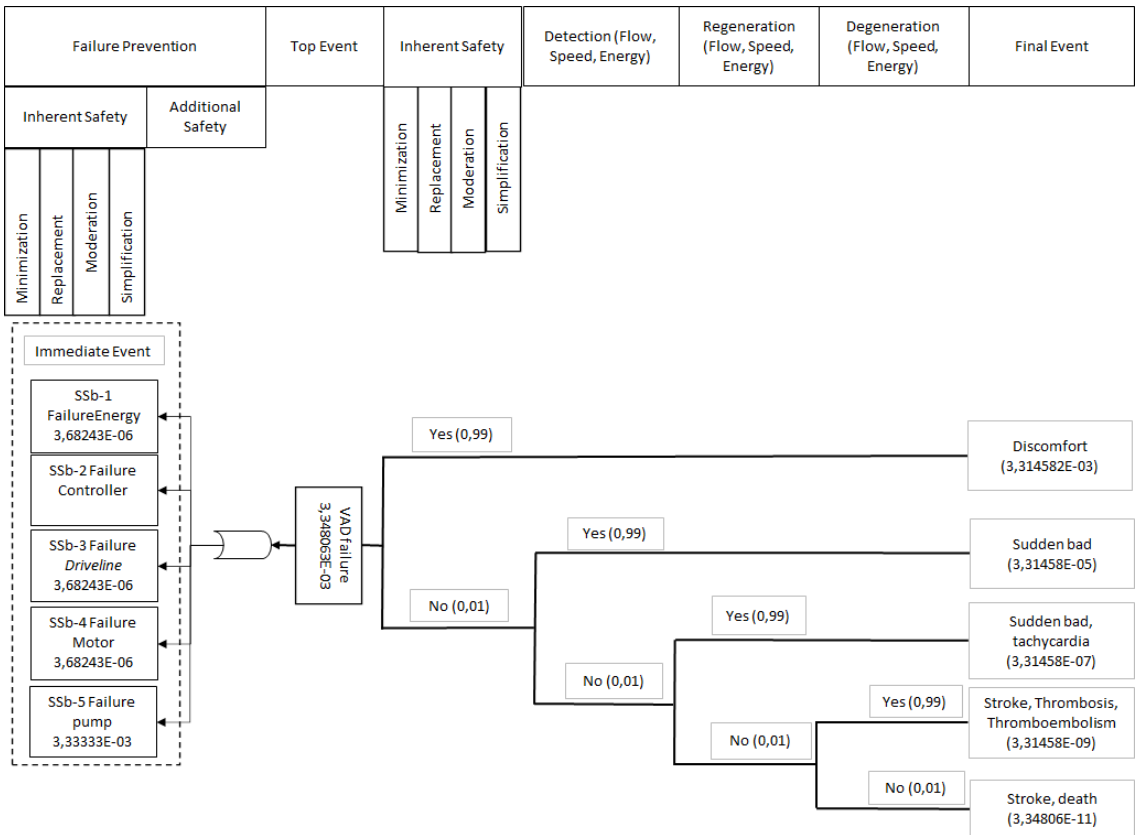


Figure 9 - Bow Tie Analysis Diagram of the VAD-PETG.01 model Project

Fonte: Prepared by the author (DIAS, 2021)

increase in the probability of occurrence of the final events: sudden bad 4.9514582-E02; mal sudden and tachycardia 4.95146-E04; stroke, thrombosis, thromboembolism 4.95146E-06; and stroke and death 5.00147E-08.

In the Bow Tie analysis diagram of Fig. 9 on the FTA side at the top of the diagram for “Failure Prevention”, there was an increment of “Inherent Safety”. After risk analysis and risk management in applying the “Reliability Improvement Method” previously applied to the VAD-PETG.01 project sample, in the bench test, the performance of the sample improved by 300 hours, which positively impacted the “SSb-5 Pump” fault frequency for 3.33333E-03, represented in the FTA.

This result represented an improvement in reliability, reducing the TE failure frequency to 3.34806E-03, when compared to the failure frequency of the VAD-AL.01 sample, to 20 hours. The result of 300 hours was considered until the time of testing.

The “Inherent Safety” column on the right side of the diagram in the SEA, right after the “Top Event” column had a positive impact on the frequency of final events, as shown in Fig. 9. The ET failure frequency was multiplied by the inferred success or failure values of the safety barriers, where the hypothesis of 99% success versus 1% failure is estimated.

This result of the ET failure frequency of 3.34806E-03, triggered a reduction in the probability of occurrence of the final events: discomfort 3.314582E-03; sudden bad 3.31458E-05; sudden and tachycardia 3,31458E-07; stroke, thrombosis, thromboembolism 3,31458E-09; Stroke and Death 3,34806E-11.

The RIIT expresses the variation between EFR by the EFA values represented in Equation 48, by the sum of the Recent Final Events, Σ_{FER} , and by the sum of Previous Final Events, Σ_{FE} . Com a aplicação de Bayesian Networks, between time t and time t+1, the

impact on the overall risk of the project can be calculated, by the variation of probabilities between the previous and the recent project, as shown in Fig. 10.

The Fig. 10 shows two moments of the project: before the AR to improve the total risk of the previous project (VAD-AL.01) and, after the Inherent Safety increment, for the component that failed and obtained an inherent safety increment for increase in the MTTF of the present project (VAD.PETG.01).

Thus, the ET is influenced by the immediate failure in the pump subsystem, SSb-4, represented in Fig. 10. As its failure probability was 5.00E-02, which is higher, the TE failure probability became 5.00147E-02 and, consequently, influenced all final events from E1 to E4, as seen in Fig. 10.

The calculations between the VAD.AL-01 sample and the VAD.PETG-01 sample, after the Inherent Safety increment, are shown below:

$$RIIT_r = \frac{\Sigma_{FER}}{\Sigma_{FEA}} = \frac{3,31E-03}{4,95E-02} + \frac{3,31E-05}{4,95E-04} + \frac{3,31E-07}{4,95E-06} + \frac{3,31E-09}{5,00E-08} + \frac{3,35E-011}{1}$$

$$RIIT_r = 0,267$$

After obtaining the RIIT, the percentage of risk improvement was calculated between the VAD.AL-01 sample and the VAD.PETG-01 sample.

$$\%MR = 100(1 - IMR) = 100(1 - 0,267) = 73,295\%$$

After the inherent safety increase, the VAD-PETG.01 sample project has not shown any more critical or catastrophic failure during the tests, so far. In this case, after applying the RIIT, the risk improvement of the VAD project for the VAD-PETG.01 sample can be observed, in the order of 73.295%.

However, because the short test time of the VAD.PETG.01 sample is insufficient to analyze its representation in relation to its %MR, a comparative analysis is made below with the Reyes model (2014). For this, a calculation

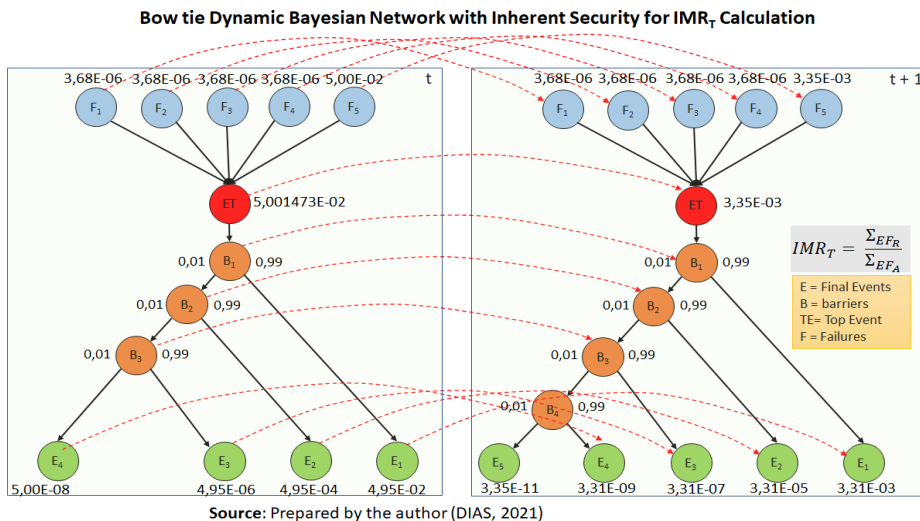


Figure 10 - Bayesian Network for IMRT calculation.

Source: Prepared by the author (DIAS, 2021)

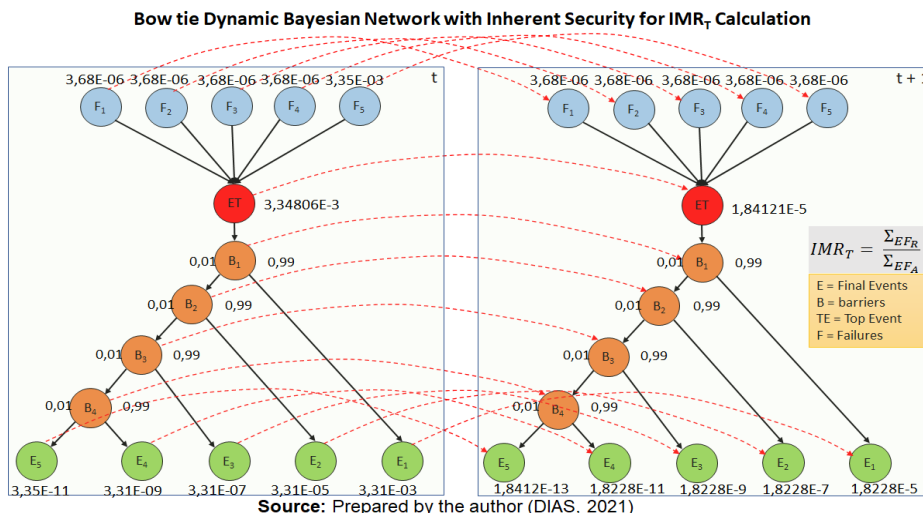


Figure 11 – Bayesian Network for calculating the IMRT between the Reyes project (2014) and VAD.PETG.01

Source: Prepared by the author (DIAS, 2021)

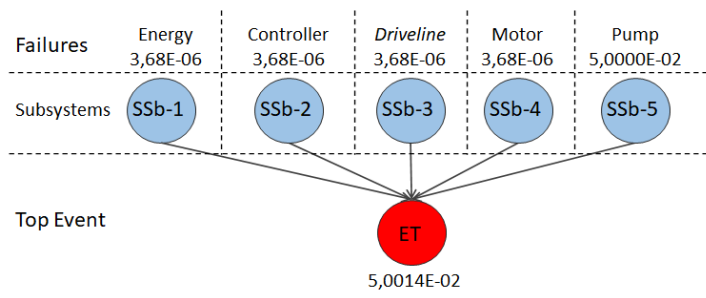


Figure 12 – Bayesian Network for representing the RII_A calculation of the VAD-AL.01 model

Fonte: Elaborado pelo autor (DIAS, 2021)

was performed, using RIIT, between the project presented by Reyes (2014) and the VAD.PETG.01 model, based on the results presented in Fig. 11.

$$RII_T = \frac{\sum_{FER} = 1,82E-05}{\sum_{FEA} = 3,31E-03} + \frac{1,82E-07}{3,31E-05} + \frac{1,82E-09}{3,31E-07} + \frac{1,82E-11}{3,31E-09} + \frac{1,84E-13}{3,35E-11}$$

$$RII_T = 0,0275$$

After obtaining the RIIT, the percentage of risk improvement was calculated between the VAD.PETG-01 model and the Reyes model (2014) tested for six years and two months without critical or catastrophic failures. This time was assumed as the intended MTBF, as a reference for this project.

$$\%RI = 100(1 - RII) = 100(1 - 0,0275) = 97,25\%$$

The result of the RII between the VAD-PETG.01 model with the %RI of 73.295% and the Reyes (2014) model that presented a %RI of 97.25% indicates the risk difference still existing in the current project to be achieved, of the order of 23.955%.

Reliability Improvement Index (RII)

The “RII” is obtained from the activity “Calculate the RII” which is based on the Bayesian Network tool. The reliability improvement index represents a quantitative analysis of the probability of occurrence of subsystem failures for the top event, between the previous design sample and the subsequent sample.

The Reliability Improvement Index (RII) obtained by the ratio between the $MTBF_A$ and the $MTBF_R$, expresses the percentage of improvement obtained between the project sample VAD-AL.01, previous project indicated by the letter “A”, and the project sample VAD-PETG.01, recent/current project indicated by the letter “R”.

The current sample, after the RA stage, was adapted with recommendations that were increased from the application of the Inherent Safety concept to failed components. For the

application of the proposed method, failure results were used during the tests of the VAD samples, performed on the test bench for the VAD-AL.01 and VAD.PETG.01 samples. We also used the results obtained in the case study by Reyes et al. (2014), as mentioned above. Thus, an intended reliability of a failure on the MTBF of six years and two months can be assumed, at which time the research was closed.

The FTA for the VAD-AL.01 sample was represented using the Bayesian Network illustrated in Fig. 12. The immediate failures in the FTA are represented with the portal “or” which leads to the participation of the sum of the immediate failures to obtain the ET. The fault frequencies for the SSb-1 Energy, SSb-2 Controller, SSb-3 Driveline, SSb-4 Motor subsystems of the VAD-AL.01 sample were 3.68E-06. The SSb-5 Pump subsystem, after testing, had a failure frequency of 5.0000E-02. Thus, the failure frequency of the ET of the VAD-AL.01 model was 5.0014E-02.

The FTA for the VAD-PETG.01 sample was represented using the Bayesian Network illustrated in Fig. 12. The immediate failures in the FTA are represented with the portal “or” which leads to the participation of the sum of the immediate failures to obtain of ET. The failures of the SSb-1 Energy, SSb-2 Controller, SSb-3 Driveline, SSb-4 Motor subsystems were inferred from the study by Reyes et al (2014) mentioned above, which resulted in a failure frequency of 3.68E -06 for each subsystem. The SSb-5 Pump subsystem failure frequency obtained during the bench tests was 3.3334E-03. The ET failure frequency of sample VAD-PETG.01 resulted in 3.3480E-03.

The RII is a ratio between the result of the reliability of the recent project over the previous project, as shown below.

$$RII_T = \frac{\frac{1}{MTBF_R} = 3,3480E-03}{\frac{1}{MTBF_A} = 5,0014E-02}$$

$$RII_T = 0,068$$

After obtaining the RII, the percentage of reliability improvement was calculated between sample VAD.PETG-01 and sample VAD.AL-01.

$$\%RI = 100(1 - RII) = 100(1 - 0,068)$$

$$\%RI = 93,20\%$$

However, as mentioned in the previous item, the testing time for the VAD.PETG.01 sample was insufficient to analyze the representativeness of its %RI. For this reason, the reliability calculated for the Reyes model (2014) was used. Thus, a calculation was performed, using the RII, between the project presented by Reyes (2014) and the sample VAD.PETG.01, based on the results shown in Fig. 12.

$$RII_T = \frac{\frac{1}{MTBFR}}{\frac{1}{MTBFA}} = \frac{1,8230E-05}{3,3480E-03}$$

$$RII_T = 0,005361$$

After obtaining the RII, the percentage of reliability improvement was calculated

between the Reyes (2014) sample and the VAD.PETG-01 sample.

$$\%RI = 100(1 - RII) = 100(1 - 0,005361) = 99,6438\%$$

$$\%RI = 99,6438\%$$

The result of the RIIT between the VAD-PETG.01 sample with the %RI of 93.20% and the samples from Reyes (2014) which presented a %RI of 99.6438% indicates the difference in reliability that still exists in the current project. be achieved, in the order of 6.4438%.

Acceptability Criteria

Once the results of the “RII” and “HII” indexes are obtained, the activity “Plot the Probability Results of Failures by the Number of Critical and Catastrophic Failures” is followed. In this step, it is possible to represent the results obtained in the “Acceptability Criteria” chart. Each tested sample presents a failure frequency by the number of catastrophic or critical failures for each tested model.

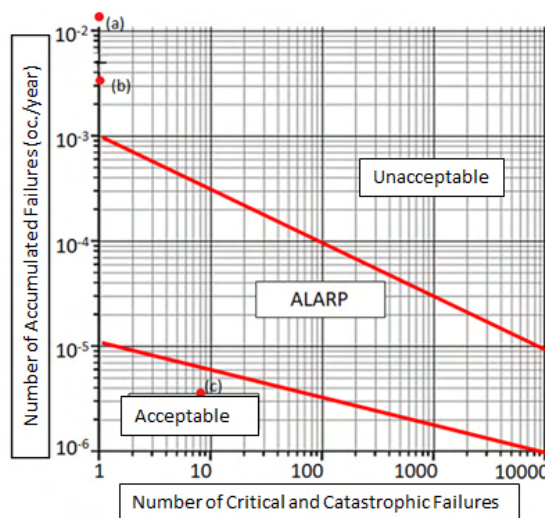


Figure 13 - Acceptability Criterion presented as a Failure Frequency by the No. of Critical and Catastrophic Failures - “FF-NFCC curve”

Source: Adapted from (MODARRES, 2006)

The tested samples VAD-PETG.01 and VAD-PETG.02, represented with the letters (a) and (b), in Fig. 13 had the fault frequencies $5.0014E-02$ and $3.3480E-03$, respectively, located in the unacceptable region, in view of the low MTBF presented. The VAD-PETG.02 sample had its MTBF measured up to the moment of this article, demonstrating better performance than the VAD-PETG.01 sample. The third point, represented by letter (c), from VAD-REYES 2014 sample used as a reference for the case study, presented a frequency of failures, of $1.8230E-05$ considering the project's MTTF of six years and two months without failures critical or catastrophic. In this case, the sample was in the "Acceptable" region, demonstrating the applicability of the proposed method.

CONCLUSIONS

The application of the proposed method results consistent with the technological innovation applied to improve life. The VAD sample VAD-PETG.01, with a failure frequency of $5.0014E-02$, was plotted in the unacceptable region. The VAD-PETG.02, until the moment of the research, had its frequency of failure considered $3.314E-03$, also unacceptable. The eight pumps from the case study by Reyes et al., (2014), which ended the project at 6 years and 2 months, were used in this project to test and validate the acceptability criterion method and had the frequency of failures of $1.8228E-05$, plotted in the acceptable region. For this project, the MTTF of 6 years and 2 months was defined as, intended MTTF.

To quantify the improvement in reliability, after defining the method for calculating the RII, it is possible to calculate the percentage of improvement between the VAD-PETG-01 and VAD-PETG.02 samples. The data obtained from the FTA were used to calculate the RII, which resulted in 0.064. The percentage of

reliability improvement between the VAD-PETG.01 sample and the VAD-PETG.02 sample was 93.20%. This result indicates that reliability needs to be improved when compared to the VAD-REYES 2014 sample, which presented an RII of 0.0003646 and a $\%RI = 99.46\%$.

On the other hand, there was also an evolution in the samples, from the treatment of the failure of the initial sample, VAD-PETG.01, which had presented a rotor lock due to constructive failure of the bearing cradle. This failure was the starting point for the application of the second stage of the research method, the Risk Analysis (as mentioned in section 2), which allowed the identification and treatment of the causes of the failures indicated. In the analysis, adjustments were suggested for the treatment of identified failures (Table 1, section 3) for the VAD-PETG.02 sample, applying the concept of Inherent Safety.

REFERENCES

- ARAKI, S. Y. et al. Friction in micro bearings of an Implantable Centrifugal Blood Pump. 2017.
- AYYUB, B. M. **Vulnerability, Uncertainty, and Risk: Analysis, Modeling, and Management**. Reston: ASCE American Society of Civil Engineers, 2011.
- AYYUB, B. M.; MCCUEN, R. H. **Probability, Statistics, and Reliability for Engineers and Scientists, Third Edition**. 3rd Editio ed. New York: CRC press, 2012.
- HERNANDES, M. M. A. P. **Análise de Escoamento em um Dispositivo de Assistência Ventricular**. [s.l.] Instituto Federal de Educação, Ciência e Tecnologia de São Paulo, 2018.
- KLETZ, T.; AMYOTTE, P. **Process Plants: A Handbook for Inherently Safer Design**. second edi ed. London: CRC press, 2010.
- KORMOS, R. L. et al. Left ventricular assist device malfunctions: It is more than just the pump. **Circulation**, v. 136, n. 18, p. 1714–1725, 2017.
- LEACH, R. **Characterisation of Areal Surface Texture**. London: Springer London, 2013.
- MASTORIS, I.; KHASHAB, M. EL; ABICHT, T. Peripheral component malfunction of a fully magnetically levitated centrifugal pump masquerading as pump thrombosis. **The Journal of Heart and Lung Transplantation**, v. 38, n. 9, p. 1000–1002, set. 2019.
- MAVROUDIS, C.; KIRKLIN, J. K.; DECAMPLI, W. M. Incremental History of the Congenital Heart Surgeons' Society (2014-2018). **World journal for pediatric & congenital heart surgery**, v. 9, n. 6, p. 668–676, 2018.
- MODARRES, M. **Risk Analysis in Engineering - Techniques, tools and Trends**. New York: CRC press, 2006.
- MODARRES, M.; KAMINSKIY, M. P.; KRIVTSOV, V. **Reliability Engineering and Risk Analysis - A Practical Guide**. Third Edit ed. New York: CRC press, 2017.
- RATHNAYAKA, S.; KHAN, F.; AMYOTTE, P. Risk-based process plant design considering inherent safety. **Safety Science**, v. 70, p. 438–464, 2014.
- REYES, C. et al. Six-year in-vitro reliability results of the heartware hvad pump. **ASAIO Journal**, 2014.
- SOLTANI, S. et al. Design changes in continuous-flow left ventricular assist devices and life-threatening pump malfunctions. **European Journal of Cardio-thoracic Surgery**, v. 47, n. 6, p. 984–989, 2014.
- SUMMERS, A. Inherently Safer Automation. **Process Safety Progress**, 2018.
- SUNDBOM, P. et al. Sound analysis of the magnetically levitated left ventricular assist device HeartMate 3™. **International Journal of Artificial Organs**, 2019.
- THEISZ, V. **Medical Device Regulatory Practices - An International Perspective**. Singapore: Pan Stanford Publishing Pte. Ltd., 2015.